

Uncertainty Quantification of RELAP5/MOD3/KAERI on Reflood Peak Cladding Temperature

Chan-Eok Park, Bub-Dong Chung, Young-Jin Lee, Guy-Hyung Lee,
and Sang-Yong Lee

Korea Atomic Energy Research Institute

(Received January 28, 1994)

재관수 첨두 피복재 온도에 대한 RELAP5 / MOD3 / KAERI의 불확실성 정량화

박찬익 · 정법동 · 이영진 · 이규형 · 이상용

한국원자력연구소

(1994. 1. 28 접수)

Abstract

The predictability of KAERI version of RELAP5/MOD3 on reflood peak cladding temperature during large break loss-of-coolant accident is assessed against 18 test runs in FLECHT SEASET test data. The associated uncertainty is statistically quantified. The selected test runs include a gravity feed test and several forced feed tests with wide range of the parameters such as flooding rate, system pressure, initial clad temperature, rod bundle power. The results show that the code under-predicts the peak cladding temperature by 7.56 K on average. The upper limit of the associated uncertainty at 95% confidence level is evaluated to be about 99 K, including the bias due to the under-prediction.

요 약

FLECHT SEASET 실험 데이터를 사용하여 대형 냉각재 상실 사고시 재관수 첨두 피복재 온도에 대한 RELAP5/MOD3/KAERI의 예측능력을 평가하였으며, 관련 불확실성을 통계적으로 정량화 하였다. 중력구동 재관수 실험 및 광범위한 재관수율, 시스템 압력, 초기 피복재 온도, 연료봉 출력을 포괄하는 강제구동 재관수 실험들로 구성된 18개의 실험이 평가에 사용되었다. 평가 결과 재관수 첨두 피복재 온도에 대해 평균 7.56 K 낮게 예측하였으며 이를 포함한 관련 불확실성의 상한은 95% 신뢰도 수준에서 약 99 K로 정량화 되었다.

1. Introduction

Recently Korea Atomic Energy Research Institute (KAERI) has modified RELAP5/MOD3 version 3.1

to solve the following problems identified through the assessment against FLECHT SEASET test data [1, 2]:

- 1) high pressure spikes and oscillation during reflood

- 2) delayed quenching
- 3) inappropriate void profile and vapor cooling in dispersed flow

The KAERI version of RELAP5/MOD3, RELAP5/MOD3/KAERI, has several improved reflood models and correlations including critical heat flux, transition boiling, and film boiling heat transfer models. It also newly incorporates wall vaporization smoothing and water level tracking model. RELAP5/MOD3/KAERI was shown to improve the predictability on reflood during large break loss-of-coolant accident(LBLOCA), in terms of peak cladding temperature(PCT), quenching time, steam temperature, and other thermo-hydraulic parameters. Further details can be seen in the reference [3].

In this study, we focus our concern on assessing the reflood PCT predictability of RELAP5/MOD3/KAERI during LBLOCA and quantifying the associated uncertainty applicable to an LBLOCA realistic evaluation model(REM). For uncertainty quantification there should be a sufficiently large number of available test data so that a statistical treatment may be possible, and the pool of data should cover the conditions expected to occur during LBLOCA. FLECHT SEASET test is chosen because the test facility is full sized with respect to axial height and experiments were performed on wide ranges of test conditions. We compare the experimental and calculational PCTs for the forced and gravity feed reflooding of 161 rod unblocked bundle tests with variations of the parameters such as flooding rate, initial clad temperature, rod peak power, and system pressure. The code uncertainty evaluated from data comparison with the relevant experimental data could be an estimate of the uncertainty attributable to the combined effect of the reflood models and correlations in the code, RELAP5/MOD3/KAERI.

2. Test Description and Simulation

2.1. Description of FLECHT SEASET Test

Forced feed experiment

The facility consists of low mass housing test section, upper and lower plena, and the related instruments and control systems. The electrically heated rods have the typical configuration of a full length Westinghouse 17×17 rod bundle. The axial power has the chopped cosine profile. The following is a brief description of procedure of the tests.

- 1) The test section is heated while empty to slightly above the saturation temperature corresponding to the test run pressure, and pressurized to the desired value by valving a boiler into the system.
- 2) The rods are allowed to heat up, until the temperatures in any two designated bundle thermocouples reach the preset value. At that time a computer automatically initiates to flood and control power decay
- 3) The exhaust control valve regulates the system pressure at a preset value by releasing steam to the atmosphere. Reflood flow is injected at the bottom of the test section.

Gravity feed experiment

The test section is the same as in the forced feed

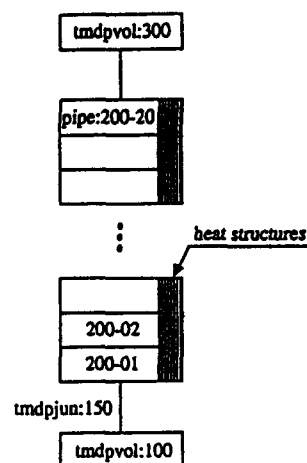


Fig. 1. Nodalization of Forced Feed Reflood Test

tests, but downcomer and the related piping are added. The feed flow is injected at the bottom of downcomer in this case. The gravity reflood tests are performed with the same procedure as in the forced reflood tests with the following exception: after flood is initiated, the flooding rate is adjusted if necessary to assure that the level in the downcomer does not go past the 4.88m elevation.

2.2. Computer Simulation

Forced feed test

The RELAP5/MOD3/KAERI is used for the simulations of FLECHT SEASET tests. The test section is modeled as one channel with 20 hydro-cells and several heat structures modelling heater rod bundle, housing, thimbles, fillers, and failed rods. The lower and upper plena are modeled as time-dependent volumes with the time-dependent conditions extracted from experimental data. Time-dependent junction connecting the time dependent volume of lower plenum to the core pipe is used to control the reflood injection velocity. The nodalization is shown in Fig. 1. The spacer grids are considered in the calculation of head loss. The heat-up and reflood phase of tests are simulated by one-through transient calculation by using the experimental heat-up and decay power data. The initial conditions are determined by the experimental clad surface and steam temperatures just before heat-up phase. The reflood feed is initiated when the heater rod power starts to decay. In the simulation of tests with radial power distribution, the heat structures are divided into three regions and a different power table is given to each region, but the corresponding hydro-cell remains a single channel.

Gravity feed test

The nodalization of gravity feed tests is shown in Fig. 2. The core is nodalized in the same manner as in the forced feed case. The downcomer is modeled as a pipe with 10 cells. The experimental reflood in-

jection flow rate is applied to the time-dependent junction connected to the bottom of the downcomer with the constraint that flow can be accumulated in the downcomer only up to a specified maximum level. Calculation is performed in the same way as in the forced feed reflood tests: one-through calculation of heat-up and reflood phase, initial condition using the experimental data at early heat-up phase, reflood feed trip at starting time of power decay, division of heater rod bundle according to the power distribution.

3. Results and Discussion

3.1. Assessment

The experimental data for the assessment are selected from the 161-rod FLECHT SEASET

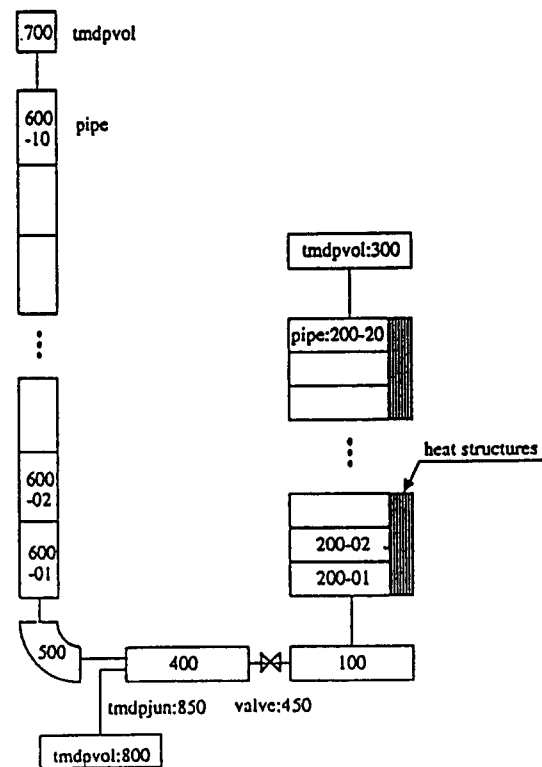


Fig. 2. Nodalization of Gravity Feed Reflood Test

reflood test data in the data bank of USNRC, ENCOUNTER[4]. The raw data consist of 177 heater rod surface temperatures, steam probe temperatures, rod bundle powers, flow rates, and absolute and differential pressures. The failed data in the total 256 channels are determined and rejected in the assessment. Linear interpolation of calculation results is necessary to correctly compare calculational and experimental data at the same elevation. The 18 selec-

ted test runs with wide range of several parameters including flooding rate, system pressure, initial clad temperature, rod bundle power, and others, are divided into 5 groups designed to investigate the effect of each parameters as shown in table 1, and described below.

Group 1 – Effect of Flooding Rate

Three planes of test section are chosen for the

Table 1. Test Matrix for Assessment

Group	Run	System Pressure (M Pa)	Rod Initial Temperature (°C)	Rod peak power (kW/m)	Flooding rate (mm/sec)	Coolant temperature (°C)	Radial power distribution	Remark
1. Flooding rate	31203	0.28	872	2.3	38.4	52	Uniform	(1)
	31302	0.28	869	2.3	76.5	52	Uniform	
	31504	0.28	863	2.3	24.6	51	Uniform	(2)
	31701	0.28	872	2.3	155.0	53	Uniform	
	31805	0.28	871	2.3	21.0	51	Uniform	
2. System pressure	31504	same as (2)						
	32013	0.41	887	2.3	26.4	66	Uniform	
	34209	0.14	889	2.4	27.2	32	Uniform	
3. Initial clad temperature	30518	0.28	256	2.3	38.9	52	Uniform	
	30817	0.27	531	2.3	38.9	53	Uniform	
	31203	same as (1)					Uniform	
4. rod bundle power	34420	0.27	119	2.4	38.9	51	Uniform	
	31021	0.28	879	1.3	38.6	52	Uniform	
	31203	same as (1)						
5. Others	34524	0.28	878	39.9	39.9	52	Uniform	
	31108	0.13	871	2.3	79.0	33	Uniform	
	32235	0.14	888	2.3	165.8(5 sec)	31	Uniform	variable flooding rate
					24.9(20 sec)			
					15.7 onward			
	32333	0.28	889	2.3	162(5 sec)	53	Uniform	variable flooding rate
					21 onward			
	33338	0.28	871	2.3	5.9 kg/s (hot)	52	Hot/cold channels	gravity feed test
34006	0.27	882	1.3	0.807 kg/s (cold)	51	Uniform		
				15				
				onward				
36026	0.28	900	2.42	25	51	FLECHT	Distributed radial power	
			2.31					
			2.19					

comparison of calculated and experimental cladding temperatures in the test run 31701: low plane(at 48 inch elevation), mid plane(at 72 inch elevation), and high plane(94 inch elevation). Fig. 3 shows the clad temperature comparisons at low, mid, and high planes. The experimental data at the same elevation except the failed channel data are averaged to be compared with the corresponding calculational value. The thicker line represents the averaged experimental cladding temperatures at the elevation, and the thinner line represents the corresponding calculational values. Calculation shows very good agreement with the experiment at mid plane, but tends to over-predicts the cladding temperatures at low and high planes. However it is noted here that the experimental data show a broad spread especially in the low and high region of test section. Fig. 4 compares the non-averaged experimental and calculational cladding temperatures at high plane. The line marked

with solid square shows calculational value and the others represent experimental data. It can be seen that the predicted clad surface temperatures are within the scattered band of the experimental data. Therefore we can conclude that slight over-prediction of peak cladding temperature(PCT) shown from the curves for low and high planes in Fig. 3 is acceptable, and that RELAP5/MOD3/KAERI code well predicts the cladding temperature in the entire core for the high flooding rate experiment, 31701. Fig. 5 shows the comparison of calculational and averaged experimental cladding temperatures at mid plane for various flooding rate. Calculation agrees well with the experiment in medium flooding rate(test runs, 31302 and 31203), but slightly underestimate the PCT in low flooding rate(test runs, 31504 and 31805). And the underprediction of PCTs in low flooding rate results from the early turn-around as shown in that figure.

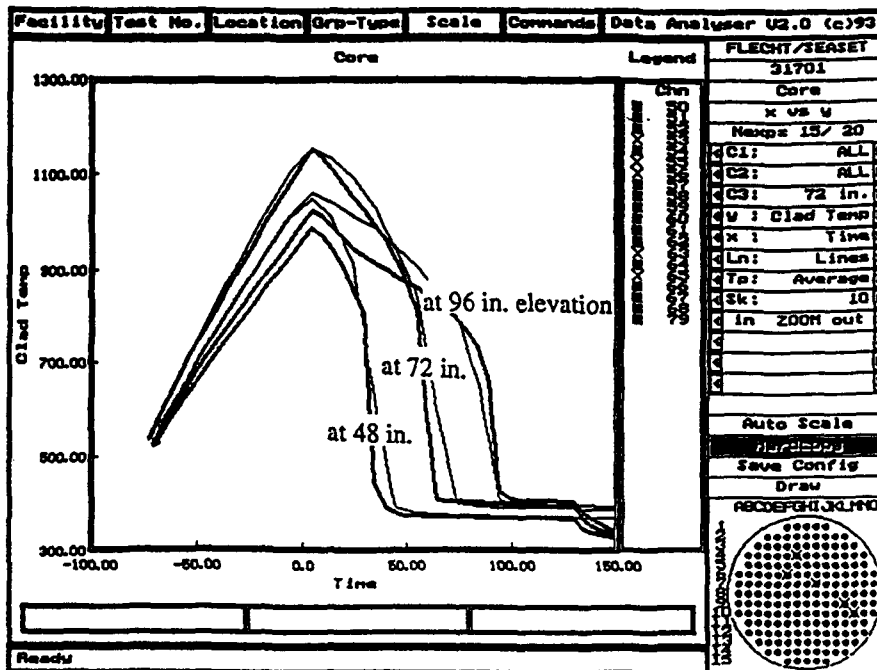


Fig. 3. Comparison of Calculational and Experimental Cladding Temperatures at Selected Elevations for Test Run. 31701

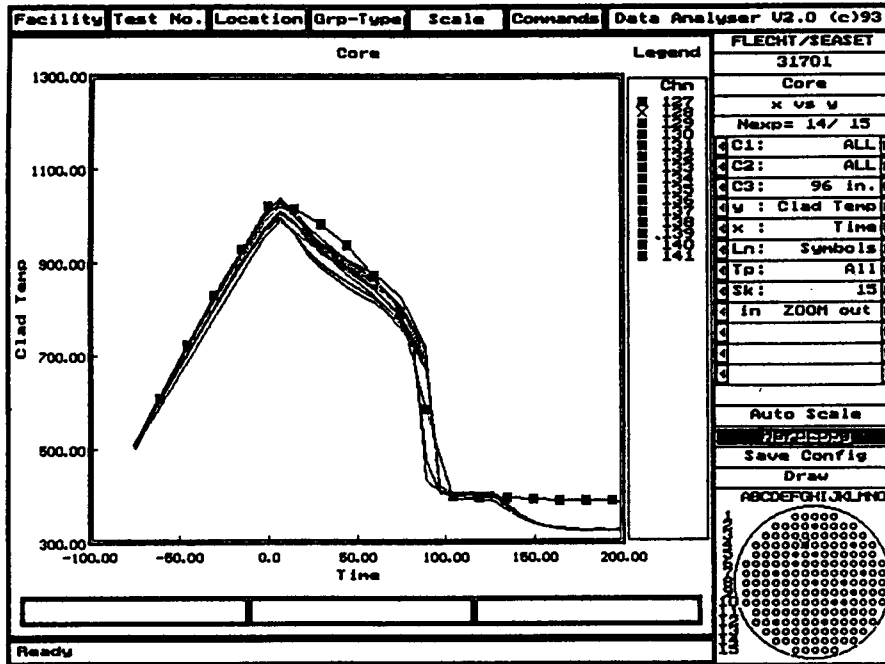


Fig. 4. Comparison of Calculational and Non-Averaged Experimental Cladding Temperatures at 96 inch Elevation for Test Run, 31701

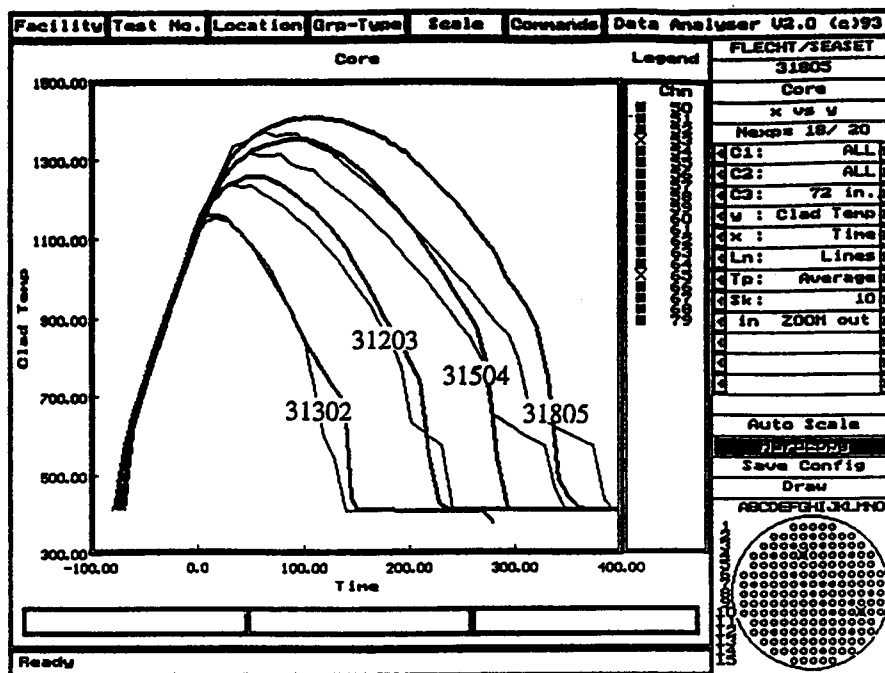


Fig. 5. Comparison of Calculational and Experimental Cladding Temperatures at 72 inch Elevation for Test Runs, 31302, 31203, 31504, and 31805

Group 2—Effect of System Pressure

The test run, 31504 has been discussed in group 1, but the results of the test runs, 32013 and 34209 are represented in Fig. 6. The calculational PCTs agree well with the experimental values both in the low and in the high pressures, but quenching is delayed in low pressure test, 34209. Then the delayed quenching may result in the over-prediction of PCT in the down stream of core.

Group 3—Effect of Initial Clad Temperature

Experimental and calculational clad surface temperatures are compared in Fig. 7 for the test runs, 34420, 30817, and 30518. The test run 31203 was already discussed in group 1. Somewhat early quenching appears in low initial clad temperature as shown in the curves for the test run, 30518, but PCTs are little impacted by the early quenching.

Therefore PCTs are well predicted even with the variation of initial clad temperature.

Group 4—Effect of Rod Bundle Power

The test runs, 31021 and 34524 are presented in Fig. 8. The test run 31203, which belongs to group 1 as well, is omitted here. The tests in the group 4 commonly show early turn-around behavior because of the low flooding rate. Quenching is delayed in high power as shown in the curves of test run, 34524, and it may result in over-prediction of PCT in the top region of core.

Group 5—The Other Effect

The test run, 36026 is selected to analyze the effect of radial power distribution. It can be seen from the comparison of computational and experimental data in the radial high power region that the radial power distribution has no significant impact on PCT prediction. However, probably because the flooding rate is low, the code under-predicts the turn-around time. In the test runs, 32333 and 32235, the flooding rate is varied during the transient. The

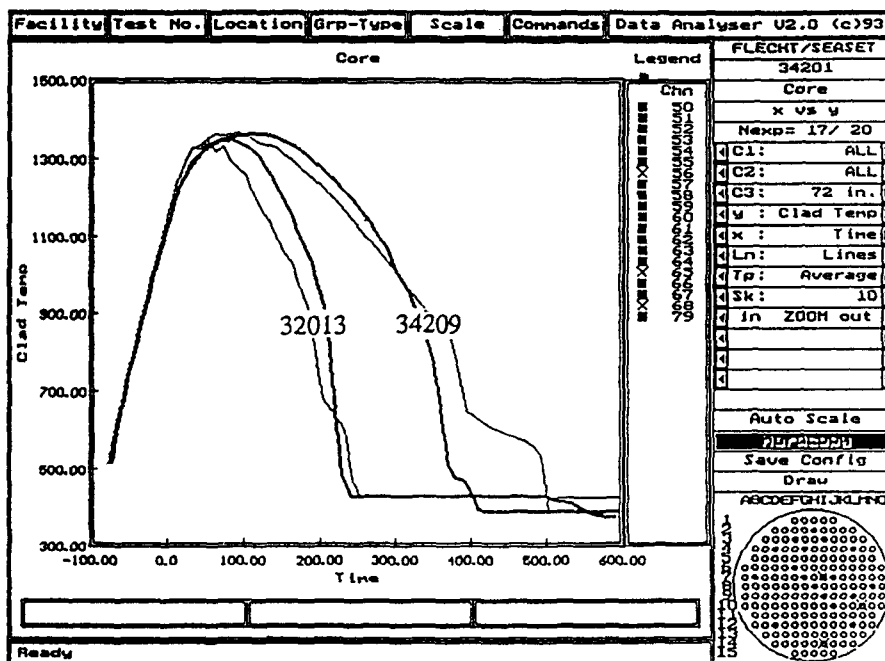


Fig. 6. Comparison of Calculational and Experimental Cladding Temperatures at 72 inch Elevation for Test Runs. 32013 and 34209

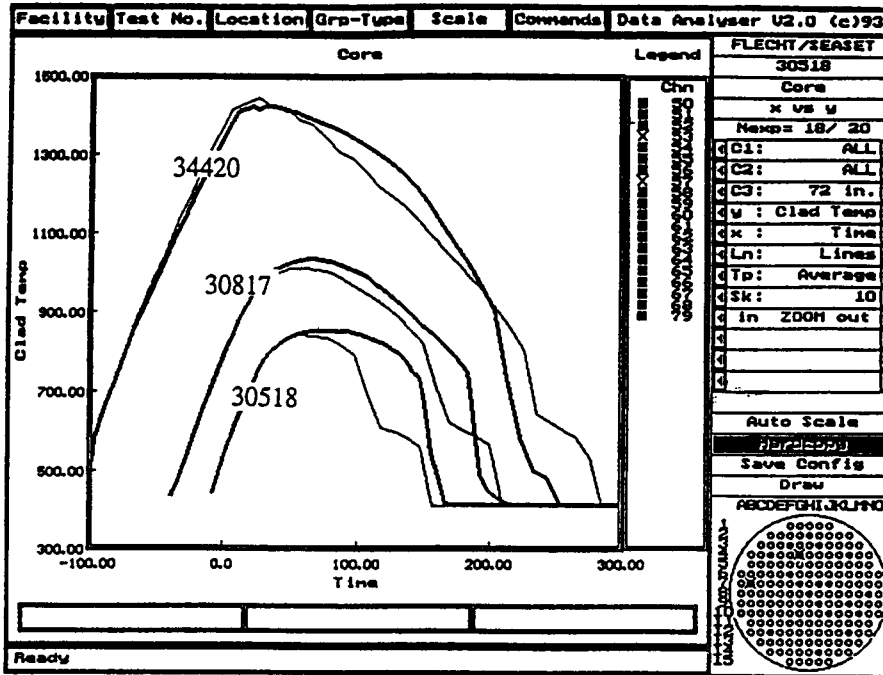


Fig. 7. Comparison of Calculational and Experimental Cladding Temperatures at 72 inch Elevation for Test Runs, 30518, 30817 and 34420

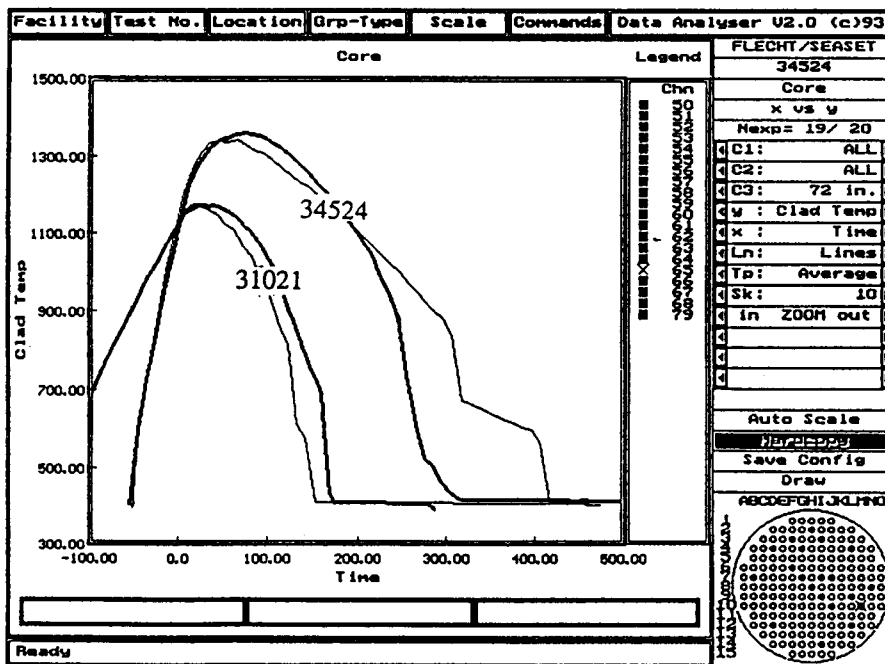


Fig. 8. Comparison of Calculational and Experimental Cladding Temperatures at 72 inch Elevation for Test Runs, 31021 and 34524

RELAP5/MOD3/KAERI predicts well the PCTs even for the variable flooding rates. The delayed quenching in test run, 32235, does not seem to be due to variable flooding rate, but due to the low system pressure. The test run, 31108, is performed in low pressure and at medium flooding rate. The calculation shows good agreement with the experimental data. The low pressure does not delay the quenching in this test in contrast to the low flooding rate cases. The test run 34006 is characterized by low rod bundle power and low flooding rate. Early turn-around of clad surface temperature and early quenching appear in that test. These trends become more severe and result in large under-prediction of PCT in top region of core. The comparison plots for the test runs, 36026, 32333, 32235, 31108, and 34006, which were discussed above, are omitted here for brevity. The gravity feed test, which is closer to the reflood conditions, is conducted in test run,

33338. Radial power distribution is also allowed in this test. The predicted clad surface temperatures in the radially hot region are compared with the corresponding experimental values in Fig. 9. The behavior of cladding temperature including turn-around time, quenching time, and PCT, agrees well with experiment in entire test section.

3.2. Uncertainty Quantification of PCT

Definition of PCT Uncertainty

PCT is generally defined as the maximum of clad surface temperatures in the entire core region during the whole transient history. However this definition would require too many simulations in order to carry out statistically meaningful quantification of the uncertainty of PCT, because it produce only one value in a test run. We notice here that the clad surface temperature at PCT location is not the only import-

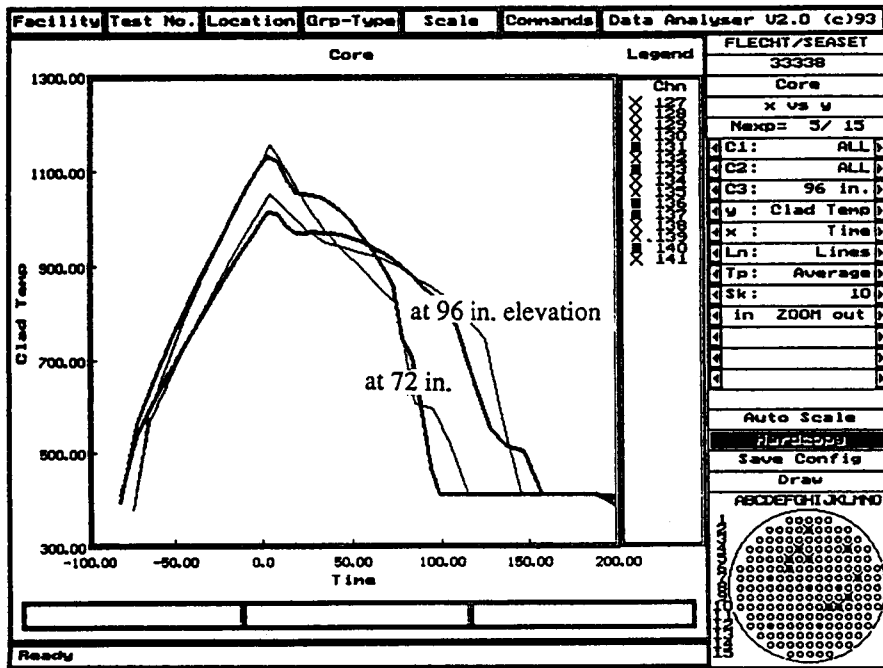


Fig. 9. Comparison of Calculational and Experimental Cladding Temperatures at Selected Elevations for the Gravity Feed Test, 33338

ant value, but those at other locations are also important to assess the code predictability of PCT. For practical purpose, PCT is then defined in this study as the local maximum value at a location of probe during the transient. Deviation between calculational and experimental PCTs is defined as follows.

$$\Delta PCT_z = PCT_{z,exp} - PCT_{z,cal} \quad (1)$$

where subscripts, z means an elevation and subscript, z_i means each measuring probe at the same elevation. In other word, the highest temperature calculated by RELAP5 for a computational cell is paired with the highest temperature measured by a probe in that cell. Many thermo-couples share each computational cell, and the center of cell do not always coincide with the measurement location. Thus the linear interpolated calculational results at certain elevation are compared with the experimental data at that elevation. PCT bias is calculated by averaging all the available ΔPCT_z for assessment test matrix, and the upper limit of uncertainty of PCT at 95% confidence level is calculated by addition of the PCT bias, μ , to 1.645 times standard deviation, σ , of all the ΔPCT_z under the assumption of normal distribution.

$$\Delta PCT = \mu + 1.645\sigma \quad (2)$$

Uncertainty Quantification

Figs. 10 to 14 show respectively the scatter diagram of PCTs for each test group. The x-axis represents PCT predicted by the code, and the y-axis does the experimental PCT. In these figures the solid line is the line of PCT bias, and the dashed line the upper limit of PCT at 95% confidence level. For the group 1, which is constructed to investigate the effect of flooding rate, the code under-predicts PCT by 18.65 K when compared with the averaged experimental PCT. The under-prediction of PCT is mainly due to the early turn-around in the tests with low flooding rate (test runs, 31504 and 31805). The uncertainty of PCT for the group 1 is about 100 K, containing the 18.16 K bias. Since all the tests in group 2 have low flooding rates, they commonly

show PCT under-prediction owing to early turn-around behavior. The run, 34209, which is a low pressure test, shows the delayed quenching and associated PCT over-prediction. As a result the bias in test group 2 is about the same as in test group 1, but the uncertainty of PCT increases to about 130 K because of the combined effect of PCT under-prediction in low flooding rate and PCT over-prediction in low system pressure. In the test group 3 the code predicts well the PCT for a wide range of initial clad temperature in spite of a little early or delayed quenching. The PCT bias is 3.64 K and uncertainty at 95% confidence level is about 74 K, which are very low compared with the test group 1 and group 2. The code predicts well PCTs in test group 4 except the high power test run 34524. In this case the calculation shows delayed quenching and the consequent PCT over-prediction. The PCT bias of group 4 is -1.49 K and uncertainty of PCT is about 80 K. As discussed above, the radial power distribution, variable flooding rate, and gravity feed do not have significant effect on PCT predictability. Under-predicted in the low flooding rate tests, 36026 and 34006, and the over-predicted in the low pressure test, 32235, and the well predicted PCTs in the other tests of group 5 are all combined and shown in Fig. 14. The PCT bias is 6.78 K and the corresponding uncertainty is about 108 K.

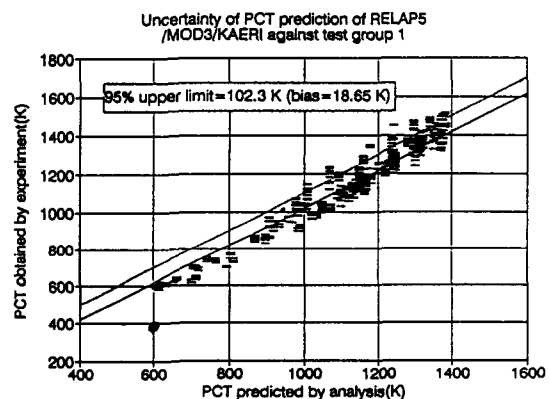


Fig. 10. Scatter Diagram of Calculational vs. Experimental PCTs for Test Group 1: Effect of Flooding Rate

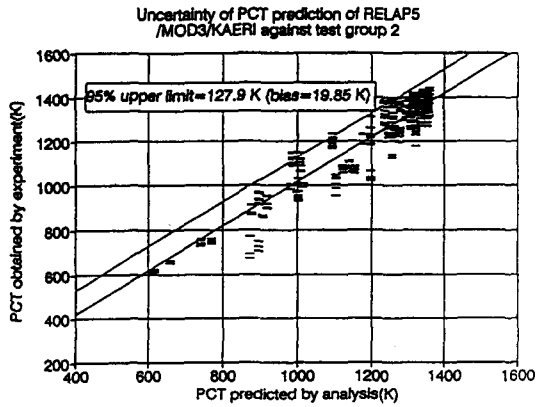


Fig. 11. Scatter Diagram of Calculational vs. Experimental PCTs for Test Group 2: Effect of System Pressure

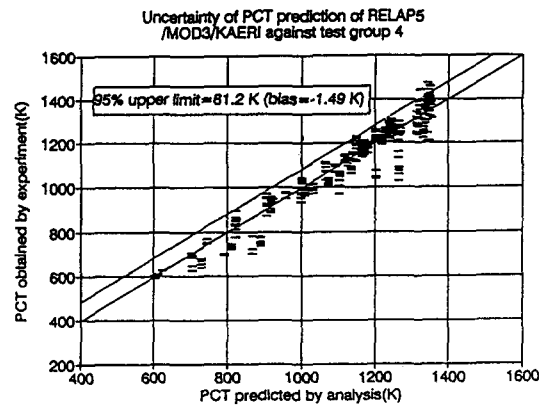


Fig. 13. Scatter Diagram of Calculational vs. Experimental PCTs for Test Group 4: Effect of Rod Bundle Power

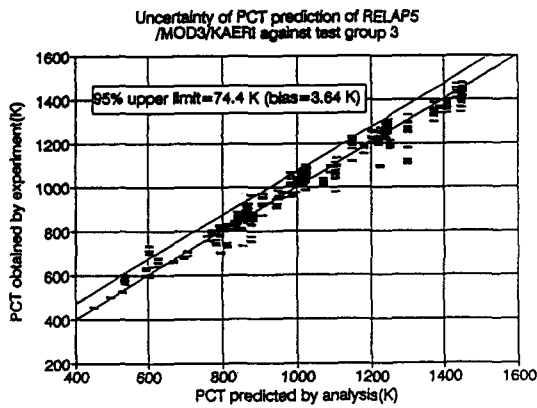


Fig. 12. Scatter Diagram of Calculational vs. Experimental PCTs for Test Group 3: Effect of Initial Clad Temperature

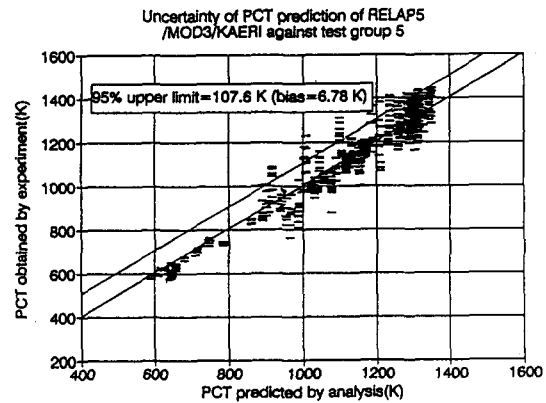


Fig. 14. Scatter Diagram of Calculational vs. Experimental PCTs for Test Group 5

We collected the data from groups 1 to 5, and constructed the scatter diagram of PCTs for all the test runs as shown in Fig. 15. The RELAP5/MOD3/KAERI code is shown to under-predict the PCTs by 7.56 K and the associated uncertainty including the bias are quantified to be 99.2 K. The validity of the assumption of normal distribution of PCTs is also checked by using the following ratio.

$$R = \frac{|\hat{P} - P|}{\sqrt{P(1 - P)}} \quad (3)$$

where \hat{P} and P respectively mean the probability and its expected value from normal distribution. The ratios are evaluated to be 0.12, 0.06, and 0.16 in the outside of the bands, $(\mu \pm \sigma)$, $(\mu \pm 2\sigma)$, and $(\mu \pm 3\sigma)$, respectively, where μ denotes mean value and σ denotes standard deviation. Thus the assumption of normal distribution is valid because all the above ratios satisfy the general criteria, $R < 3$ [5].

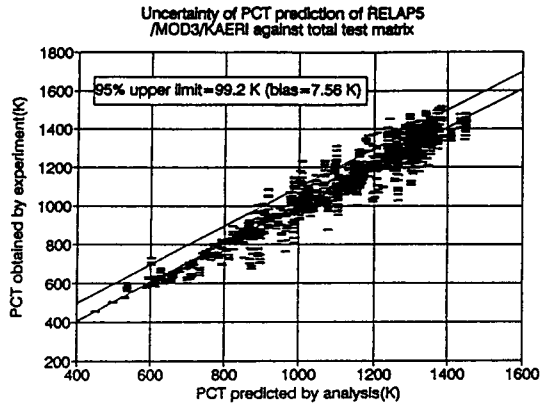


Fig. 15. Scatter Diagram of Calculational vs. Experimental PCTs for Total Test Matrix

4. Conclusion

The KAERI modified version of RELAP5/MOD3 is assessed against FLECHT SEASET test data with the wide ranges of several parameters: 15 to 155 mm/sec flooding rate, 0.13 to 0.41 MPa system pressure, 256 to 1119°C initial clad temperature, and 13 to 3 kW/m rod peak power. The assessment matrix include a gravity feed reflood test as well as forced feed tests with and without variable flooding rate. Radial power distribution is also allowed in some test runs including the gravity feed test. The code is found to predict generally well the thermal hydraulic behaviors including PCT at heat-up and reflood phase during LBLOCA, in spite of the following exceptions:

1. Slight under-prediction of PCT in low flooding rate due to early turn-around of clad temperatures
2. Delayed quenching in the tests with low pressure and low flooding rate and in the tests with high power, and the consequent over-prediction of

PCT at top region of core

3. Early quenching in the test with low power and low flooding rate, and the consequent under-prediction of PCT at top region of core

The scatter diagram of PCTs is made from the comparison of all the calculational PCTs and the corresponding experimental values. 2793 data in form of deviation between experimental and calculational PCTs are shown to be normally distributed, and used to quantify statistically the PCT uncertainty of code. The upper limit of PCT uncertainty at 95% confidence level is evaluated to be about 99 K. The PCT uncertainty might be attributable to reflood models and correlations in the code and experimental data spread. As mentioned above, the used data encompass so wide ranges of parameters that they cover the conditions expected to occur at reflood phase of LBLOCA. Therefore the evaluated uncertainty of reflood PCT could be applied to realistic evaluation model of LBLOCA.

References

1. PWR FLECHT SEASET Unblocked Bundle, Forced and Gravity Reflood Task: Data Report, Volumes 1 & 2, NUREG/CR-1532 (1981)
2. PWR FLECHT SEASET Unblocked Bundle, Forced and Gravity Reflood Task: Data Evaluation and Analysis Report, NUREG/CR-2256 (1982)
3. B.D. Chung et al., "Development of RELAP5/MOD3 Reflood Model", Proceedings of Korean Nuclear Society Spring Meeting (1993)
4. NRC/DRPS Reactor Safety Data Bank, ENCOUNTER, EGG-RTH-7285
5. 김우철외, 현대통계학, 서울, 영지문화사 (1980)